Acta Oceanol. Sin., 2021, Vol. 40, No. 3, P. 46–57
https://doi.org/10.1007/s13131-021-1706-5
http://www.hyxb.org.cn
E-mail: hyxbe@263.net

An assessment of Arctic cloud water paths in atmospheric reanalyses

Mingyi Gu[1], Zhaomin Wang[2, 6*], Jianfen Wei[3, 4], Xiaoyong Yu[5, 6]

[1] School of Atmospheric Science, Nanjing University of Information Science and Technology, Nanjing 210044, China

[2] College of Oceanography, Hohai University, Nanjing 210098, China

[3] School of Environmental Science and Engineering, Nanjing University of Information Science and Technology, Nanjing 210044, China

[4] Institute for Climate and Application Research (ICAR), Nanjing University of Information Science and Technology, Nanjing 210044, China

[5] School of Marine Sciences, Nanjing University of Information Science and Technology, Nanjing 210044, China

[6] Southern Marine Science and Engineering Guangdong Laboratory (Zhuhai), Zhuhai 519082, China

Received 23 June 2020; accepted 17 August 2020

Abstract

The role of Arctic clouds in the recent rapid Arctic warming has attracted much attention. However, Arctic cloud water paths (CWPs) from reanalysis datasets have not been well evaluated. This study evaluated the CWPs as well as LWPs (cloud liquid water paths) and IWPs (cloud ice water paths) from five reanalysis datasets (MERRA-2, MERRA, ERA-Interim, JRA-55, and ERA5) against the COSP (Cloud Feedback Model Intercomparison Project Observations Simulator Package) output for MODIS from the MERRA-2 CSP (COSP satellite simulator) collection (defined as M2Modis in short). Averaged over 1980–2015 and over the Arctic region (north of 60°N), the mean CWPs of these five datasets range from 49.5 g/m^2 (MERRA) to 82.7 g/m^2 (ERA-Interim), much smaller than that from M2Modis (140.0 g/m^2). However, the spatial distributions of CWPs, show similar patterns among these reanalyses, with relatively small values over Greenland and large values over the North Atlantic. Consistent with M2Modis, these reanalyses show larger LWPs than IWPs, except for ERA-Interim. However, MERRA-2 and MERRA underestimate the ratio of IWPs to CWPs over the entire Arctic, while ERA-Interim and JRA-55 overestimate this ratio. ERA5 shows the best performance in terms of the ratio of IWPs to CWPs. All datasets exhibit larger CWPs and LWPs in summer than in winter. For M2Modis, IWPs hold seasonal variation similar with LWPs over the land but opposite over the ocean. Following the Arctic warming, the trends in LWPs and IWPs during 1980~2015 show that LWPs increase and IWPs decrease across all datasets, although not statistically significant. Correlation analysis suggests that all datasets have similar interannual variability. The study further found that the inclusion of re-evaporation processes increases the humidity in the atmosphere over the land and that a more realistic liquid/ice phase can be obtained by independently treating the liquid and ice water contents.

Key words: Arctic, clouds, cloud water paths (CWPs), reanalysis evaluation

Citation: Gu Mingyi, Wang Zhaomin, Wei Jianfen, Yu Xiaoyong. 2021. An assessment of Arctic cloud water paths in atmospheric reanalyses. Acta Oceanologica Sinica, 40(3): 46–57, doi: 10.1007/s13131-021-1706-5

1 Introduction

Since the 1980s, the Arctic has experienced rapid warming, which is a phenomenon called Arctic amplification (AA) (Screen and Simmonds, 2010; Serreze and Barry, 2011; Dethloff et al., 2019), in contrast to the situation around the Antarctic (Wang et al., 2015). To better predict long-term climate change in the Arctic, it is necessary to understand cloud processes, their interrelationships with radiation and the underlying boundary layer, as well as their impacts on the polar and global climate system (Curry et al., 1996). Although cloud representations in climate models have become increasingly sophisticated in the past three decades, the observed and simulated results still have large discrepancies, and the role of clouds in driving AA remains unclear (Kay et al., 2016).

Reanalysis systems are convenient tools for studying the Arctic climate system in such data-sparse regions where in situ observations are difficult to obtain due to the extreme and harsh environments. Specifically, an atmospheric reanalysis system employs an atmospheric general circulation model, which combines a data assimilation scheme and uses all available observations to produce a spatially complete gridded meteorological dataset (Dee et al., 2011). Users want to consider reanalysis products as equivalent to observations, but this is not always justifiable, especially in the Arctic. Uncertainties in these products should be evaluated before using these data to address scientific questions.

When considering the climatic influences of clouds, the performances of reanalyses on cloud cover and radiation properties

Foundation item: The National Key R&D Program of China under contract No. 2018YFA0605904; the Global Change Research Program of China under contract No. 2015CB953900; the Innovative Platform Program of Chinese Arctic and Antarctic Administration under contract No. CXPT2020009; the Program of China Scholarships Council under contract No. 201908320511.
*Corresponding author, E-mail: zhaomin.wang@hhu.edu.cn

have been widely evaluated. The results so far indicate that all reanalyses exhibit large biases in the cloud cover. For example, Walsh et al. (2009) examined cloud cover and radiative fluxes in NCEP R1, ERA-40, NARR, and JRA-25 through comparisons with surface data from Barrow, Alaska. They found that systematic errors in cloud cover were substantial. The cloud cover biases showed considerable variations in their annual mean and seasonal cycle. The ERA-40 cloud coverage simulation is the most realistic of the four reanalyses. Chernokulsky and Mokhov (2012) evaluated and intercompared the total cloud cover based on 16 Arctic cloud climatologies from different satellite products, surface observations and reanalyses. According to their work, reanalyses are not in a close agreement with satellite and surface observations of cloudiness in the Arctic, despite that MERRA reanalysis has the best fit to observations for annual mean total cloud cover. Liu and Key (2016) examined the performance of five atmospheric reanalysis products: ERA-Interim, MERRA, MERRA-2, NCEP R1, and NCEP R2, by depicting monthly mean Arctic cloud amount anomalies against MODIS satellite observations from 2000 to 2014 and against CALIPSO observations from 2006 to 2014. They concluded that all five reanalysis products were biased in terms of the mean cloud amount, especially in winter, while there were no significant differences in the overall performances of reanalysis products in depicting cloud amount inter-annual variability. Although ERA-40 has been found to be the most suitable for shortwave and longwave fluxes because of its most realistic cloud cover, radiative fluxes may not always depend on the cloud cover (a similar conclusion was obtained in Chernokulsky and Mokhov (2012)). Taylor et al. (2019) compared the amount and the annual cycle of Arctic cloud cover in CMIP5 with those in CALIPSO-CloudSat-derived products, MERRA-2 and ERA-Interim products. They found that the largest differences that occur between the surface and 950 hPa are attributed to cloud ice microphysical processes. Thus, cloud microphysical parameterizations drive significant inter-model differences in the amount and the annual cycle of Arctic cloud cover. Therefore, other cloud properties may also play important roles in the radiative fluxes and hence their counterparts in reanalysis datasets need to be evaluated.

In fact, for example, the cloud emissivity, an important radiative property, is usually parameterized as functions of cloud liquid water content, cloud ice content, and effective radius of cloud particles in the models (Dee et al., 2011; Kobayashi et al., 2015). The sum of the cloud liquid and ice water path (LWP and IWP) (a vertical integral of the cloud liquid and ice water content per unit area of air) is called the cloud water path (CWP). Thus, the CWP is also a variable that may affect radiative fluxes, in addition to the widely reported unreliable cloud cover. However, in the traditional concept, CWPs are more often regarded as important cloud microphysical quantities when describing the properties of clouds and their radiative effects have not been sufficiently addressed. Huang et al. (2017) compared five reanalyses—JRA-55, 20CRv2c, CFSR, ERA-Interim, and MERRA-2, and two satellite surface observations—NASA CERES–MODIS (CM)-derived cloud cover, CWPs, top-of-atmosphere and surface longwave and shortwave radiative fluxes, and CloudSat–CALIPSO-derived cloud fractions. They found that all reanalyses exhibited large negative CWPs biases in summer. Lenaerts et al. (2017) briefly compared derived LWPs and IWPs products from CloudSat–CALIPSO and CERES with ERA-Interim, MERRA-2 and 28 CMIP5 models when evaluating the polar cloud and radiation over the period of 2007–2010. Based on their results, it was shown that CWPs are underestimated in nearly all models, LWPs and IWPs biases are inconsistent between the models, precluding any conclusions on shared model deficiencies, and MERRA-2 and JRA-55 show comparatively higher correlations for the Arctic cloud and radiation properties. Rozenhaimer et al. (2018) compared airborne measurements obtained from the Arctic Radiation IceBridge Sea&Ice Experiment (ARISE) during the fall of 2014 with concurrent MERRA-2 products over the Beaufort Sea. They found that MERRA-2 has a warm near-surface temperature bias, and underestimates near-surface LWPs and IWPs over open water and sea ice surfaces.

Although some previous studies have pointed out the importance of the work on Arctic cloud and a little talked about Arctic CWPs, few of them evaluated directly on CWPs, making the knowledge of Arctic CWPs sparsely scattered and loosed. The purpose of this study is to examine the climatologies of CWPs, LWPs and IWPs in the Arctic (north of 60°N) by analyzing available global reanalysis datasets, to provide comprehensive comparisons between these products and to give a more detailed description of Arctic CWPs, LWPs and IWPs. The data we used, and their sources are introduced in Section 2. The assessment and comparison of the climatologies of CWPs, LWPs, and IWPs in different reanalysis products are presented in Section 3. The main findings are summarized in Section 4, along with some suggested future work.

2 Data

Table 1 provides a brief overview of the recent versions of the global reanalysis datasets used in this study. The CWPs in these datasets in this study are simply the sum of the LWPs and the IWPs. Reanalysis datasets that did not offer CWPs, LWPs, and IWPs products, such as CFSR, were not included in this study.

2.1 *ERA-Interim*

ERA-Interim is a reanalysis of meteorological observations produced by the European Centre for Medium-Range Weather Forecasts (ECMWF) (Dee et al., 2011). In ERA-Interim, clouds are variables modeled by prognostic equations for the cloud condensate and cloud cover, which are only indirectly constrained by the available observations of temperature and humidity (Tiedtke, 1993). The incorporation of the effects of the clouds on the longwave fluxes follows the treatment discussed by Washing-

Table 1. Datasets used in this study

Variable	ERA5	ERA-Interim	JRA-55	MERRA-2	MERRA	M2Modis
Institution/project	ECMWF	ECMWF	JMA	NASA-GSFC	NASA-GSFC	NASA-GSFC/CFMIP COSP
Resolution (lon. × lat.)	0.25°×0.25°	0.75°×0.75°	1.25°×1.25°	0.625°×0.500°	0.66°×0.50°	0.625°×0.500°
Temporal range	Jan. 1979 to present	Jan. 1979 to present	Jan. 1958 to present	Jan. 1980 to present	Jan. 1979 to Feb. 2016	Jan. 1980 to present
Cloud property parameterizations	Tiedtke (1993)	Tiedtke (1993)	Sommeria and Deardorff (1977)	Bacmeister et al. (2006)	Bacmeister et al. (2006)	

Note: See Section 2.5 for more details of M2Modis.

ton and Williamson (1977). Presently, the optical properties of clouds are based on the derivation of water clouds by Fouquart (1988) and ice clouds by Ebert and Curry (1992). The effective radius of the liquid water cloud particles was computed from the cloud liquid water content using the diagnostic formulation of Martin et al. (1994) and specific cloud condensation nuclei concentrations over land and ocean. For ice clouds, a revised formulation of Ou and Liou (1995) was used to diagnose the effective dimension of cloud particles based on temperature. The cloud optical thickness is defined as a function of spectrally varying mass absorption coefficients with the relevant cloud water and ice paths, and is used within the true cloudy fraction of the layer. Alternative sets of cloud optical properties are based on the study by Savijärvi and Räisänen (1998) for liquid water clouds, and Fu et al. (1998) for ice clouds (see ECMWF (2010) for more details).

2.2 *ERA5*

ERA5 is the latest atmospheric reanalysis dataset formed by ECMWF (Hersbach et al., 2020). Compared with ERA-Interim, the philosophy of the original scheme (Tiedtke, 1993) is still used, but is significantly modified in ERA5. ERA5 adds independent prediction equations for liquid and ice water contents, which increase moisture-related prognostic variables from three to six, thereby allowing a more physically realistic representation of the existence of super-cooled liquid water and mixed-phase cloud. (for more details, see ECMWF. IFS documentation CY41R2 Part IV, https://www.ecmwf.int/node/16648)

2.3 *JRA-55*

JRA-55 is the second Japanese global atmospheric reanalysis project conducted by the Japan Meteorological Agency (JMA), based on the JMA's global spectral model (GSM) (Kobayashi et al., 2015). In the longwave flux calculations, clouds are basically treated as blackbodies. Cloud overlap is represented by assuming the maximum-random overlap (Geleyn and Hollingsworth, 1979) with the method of Räisänen (1998). The effects of cloud cover and cloud emissivity on cloud overlap are considered separately (Kitagawa and Murai, 2006). The cloud emissivity is parameterized as functions of cloud liquid water content, cloud ice content, and effective radius of cloud particles. Cloud optical properties used in the shortwave radiation scheme, i.e., the cloud optical depth, the single scattering albedo, and the cloud asymmetry factor, are parameterized as functions of the cloud water path and effective radius of cloud particles according to Slingo (1989) for water droplets and Ebert and Curry (1992) for ice crystals (see Japan Meteorological Agency 2019, etc. for more details).

2.4 *MERRA*

NASA's MERRA dataset is based on the Goddard Earth Observing System (GEOS) Data Assimilation System (DAS) version 5.2.0 by NASA's Global Modeling and Assimilation Office (GMAO) with two primary objectives: to place observations from NASA's Earth Observing System (EOS) satellites into a climate context, and to improve upon the hydrological cycle represented in earlier generations of reanalysis (Rienecker et al., 2011). GEOS-5 includes moist physics with prognostic clouds (Bacmeister et al., 2006), which is a modified version of the relaxed Arakawa–Schubert convection scheme described by Moorthi and Suarez (1992), and the radiation scheme of Chou et al. (2001).

2.5 *MERRA-2*

MERRA-2 is a new retrospective analysis that represents an update of the original MERRA system (Gelaro et al., 2017). The model used in producing MERRA-2 is still the GEOS, but version 5.12.4. The MERRA-2 AGCM scheme for re-evaporation of precipitation and suspended cloud water and ice contains a series of new parameter settings, which lead to a substantial increase over the MERRA model in the re-evaporation of snow and ice. In comparison with MERRA, fundamental improvements in simulated climate are associated with the increased re-evaporation from frozen precipitation and cloud condensate, resulting in a wetter atmosphere. A series of resolution-aware parameters related to moist physics have been shown to be improving at higher resolutions, resulting in AGCM simulations exhibiting seamless behavior across different resolutions and applications (Molod et al., 2015).

2.6 *COSP output for MODIS*

English et al. (2014) suggested that Arctic clouds during the wintertime are too close to the surface and/or too optically thin to be observed by CALIPSO, which may lead to an unfair evaluation of the model output. Using the Cloud Feedback Model Intercomparison Project (CFMIP) Observation Simulator Package (COSP) could be chosen to make this comparison more consistent. COSP includes simulators that are compatible with the ISCCP, PARASOL, CALIPSO, CALIOP, MISR, MODIS, and CloudSat observational products. Cloud Feedback Model Intercomparison Project (CFMIP) COSP output for ISCCP and MODIS was provided by MERRA-2 in the CSP collection (Bosilovich et al., 2016). In this paper, we simply use the MERRA-2 CSP collection as the base data for the assessment. In the MERRA-2 CSP collection, CWPs are retrieved from MODIS. Hereinafter, MERRA-2 CSP is referred to as M2Modis. To obtain a consistent period for comparison, data from 1980 to 2015 were used, and all data were interpolated into the grid spacing of M2Modis (same as MERRA-2). Note that there are unobserved regions in M2Modis in wintertime, so these unobserved areas were removed when making comparisons between reanalysis datasets and M2Modis, except for seasonal cycles (see Section 3.2).

3 Results

3.1 *Mean states*

The mean climatological values and standard deviations (STD) of Arctic (north of 60°N) CWPs, LWPs and IWPs during the same period (January 1980 to December 2015) are listed in Table 2. For Arctic CWPs, different reanalyses held different mean values from 49.5 g/m^2 (MERRA) to 82.7 g/m^2 (ERA-Interim), which is much smaller than that of the M2Modis (140.0 g/m^2). This result is consistent with Huang et al. (2017) who compared the results of some reanalysis datasets with NASA CERES-MODIS CWP (126 g/m^2) in the region north of 70°N and during the period of 2000–2012. For Arctic LWPs, the situation is similar to that of CWPs, with average LWPs ranging from 29.7 g/m^2 (JRA-55) to 58.8 g/m^2 (MERRA-2), which is much smaller than 80.9 g/m^2 for M2Modis. Although IWP from ERA-Interim (43.1 g/m^2) is the closest to that of M2Modis (59.1 g/m^2), IWPs in other datasets exhibit huge biases, with JRA-55 and ERA5 IWP being lower than half of M2Modis IWP and with MERRA and MERRA-2 IWPs being even smaller than a quarter of M2Modis IWP.

The spatial patterns of CWPs, LWPs, and IWPs climatological mean values are shown in Fig. 1, and the standard deviations are shown in Fig. 2. Despite the large difference in mean values and standard deviations, the main patterns of CWPs, LWPs, and IWPs were similar, with small values over Greenland and large values over North Atlantic Warm Current (Fig. 1).

Climate models have also long been known to be sensitive to

Table 2. Means and standard deviations of LWPs, IWPs, and CWPs and the ratios of average IWPs to average CWPs over the Arctic

Reanalysis datasets	LWP/ ($g \cdot m^{-2}$)		IWP/ ($g \cdot m^{-2}$)		CWP/ ($g \cdot m^{-2}$)		$\frac{IWP}{CWP}$/%
	Mean	STD	Mean	STD	Mean	STD	
M2Modis	80.9	40.7	59.1	29.8	140.0	62.6	42
MERRA-2	58.8	24.0	13.1	5.5	71.8	25.8	18
MERRA	35.0	14.9	14.6	5.8	49.5	17.3	29
ERA5	49.0	31	22.4	8.5	71.4	35.6	31
ERA-Interim	39.6	31.0	43.1	16.3	82.7	37.9	53
JRA-55	29.7	23.7	25.1	11.6	54.8	31.1	46

cloud phase parameterizations. For example, a modeling study has shown that modifying the threshold of cloud phase conversion could change the sign of the global net cloud-climate feedback from negative to positive (Li and Le Treut, 1992). Therefore, besides LWPs and IWPs climatological mean values, the distributions of IWPs/CWPs also need to be evaluated (Table 2 and Fig. 3). As listed in Table 2, LWPs were slightly higher than IWPs over the Arctic in M2Modis; MERRA-2 and MERRA overestimated the portions of LWPs; ERA-Interim and JRA-55 overestimated the portions of IWPs. As shown in Fig. 3, for M2Modis, in most parts of the Arctic, the portions of LWPs are slightly higher than those of IWPs, while in Greenland the portions of IWPs may exceed 70%. Considering the different treatments of cloud in different reanalyses and the difficulty of cloud phase simulation, not surprisingly, the ratios of IWPs to CWPs vary significantly among these datasets. MERRA-2 and MERRA underestimated the IWPs over the entire Arctic. MERRA-2 underestimated IWPs even more seriously than MERRA. Since a warmer atmosphere retains more moisture and favors more liquid cloud water than solid cloud water, this underestimation of IWPs suggests a large warm bias in MERRA-2. ERA-Interim and JRA-55 overestimated IWPs almost throughout the Arctic, with the largest overestimation being in Greenland. ERA-Interim grossly overestimated the proportion of solid cloud water on Arctic land, with the majority overestimating by more than 20%. ERA5 underestimated IWPs throughout the Arctic except some parts of North America and Europe and whole Greenland. As described in Section 2, compared with ERA-Interim, ERA5 uses a new cloud scheme with independent liquid and ice water contents in prognostic variables, which leads to better represented ratio of ice to liquid phases. The adjusted ratio of ice to liquid phases is evident in Fig. 3. Compared to other datasets, ERA5 performed better.

3.2 *Mean seasonal cycles*

3.2.1 *Monthly mean comparison*

Here we compare the long-term monthly means of the five reanalysis datasets to those of M2Modis. As shown in Fig. 4, the seasonal cycles of CWPs, LWPs, and IWPs in these datasets are similar, despite the large differences in their values. All datasets have higher CWPs in summer than in winter controlled by the LWPs seasonal cycle. It is difficult to see consistent IWP seasonal cycles among the six datasets. For example, the IWP minimum appears in April (February) and the maximum appears in July (September) for M2Modis (JRA55). For ERA-Interim and ERA5, however, the IWP minimum appears in July and the maximum appears in October. The inconsistency in IWP seasonal cycles may reflect the inconsistency of relative influences of thermal and moisture status on IWP seasonal cycles. For ERA-Interim and ERA5, the seasonal cycles of arctic thermal status, which peaks in summer and limits the existence of solid phase cloud water, may dominate the IWP seasonal cycle. For M2Modis and JRA55, the moisture seasonal cycle may dominate the IWP seasonal cycle.

3.2.2 *Spatial distributions*

The spatial distributions of LWPs and IWPs in M2Modis are shown in Fig. 5, along with the missing areas in several winter months (October, November, December, January, and February). Unlike the mean values over the Arctic in Fig. 4, the seasonal variations of IWPs were significant in most areas for M2Modis, as shown in Fig. 5. This is because IWPs have opposite seasonal variation over land and sea. Lower in winter and higher in summer over the land, while higher in winter and lower in summer over the ocean. However, the reanalysis datasets do not show consistent seasonal cycles (not shown).

The Arctic was then divided into four sub-regions to get their regional means and seasonal cycles: Mainland (the Arctic portions of Eurasia and North America), Greenland (including Iceland), sea-ice-covered regions where climatological monthly mean sea ice concentration $\geqslant$15%, and ice-free oceans. Figure 6 illustrates these four sub-regions with the sea-ice-covered regions in March and September being determined by the average sea ice concentration (SIC) during 1980–2015 in MERRA-2. The seasonal cycles of LWPs and IWPs for these four regions are shown in Fig. 7. Over the Arctic, the LWPs in reanalysis datasets were all large in summer and small in winter except for MERRA-2 on ice-free ocean. For IWPs of M2Modis, the striking feature is that in summer, IWPs are larger over land, which is in contrast to the situation over the ocean; however, this feature is difficult to interpret since a warmer condition should lead to smaller IWPs in summer over the land. We note that there is no such feature for the five reanalysis datasets, which suggests that the IWPs may not be well understood.

3.3 *Linear trends and variability*

Similar to the question addressed in Liu and Key (2016) for cloud cover, if the average CWP in a reanalysis product exhibits bias, does that preclude its use in anomaly-based climate studies rather than absolute CWPs? To address this question, linear trends are simply compared with annual anomalies among these datasets, and then the correlations are calculated using both original and detrended time series between the reanalysis datasets and M2Modis. The results are shown in Fig. 8 and Table 3. In Fig. 8, LWPs from all datasets increased slightly, while IWPs decreased slightly. Although the linear trends are not significant except for the trend of LWPs from M2Modis (Table 3), these changes are consistent with the warming in the Arctic. In M2Modis, LWPs increase and IWPs decrease mainly in summer (not shown). Reanalysis can partially capture the differences in seasonal trends in LWPs and IWPs, but with smaller values and smaller areas of significance (not shown). In all reanalyses, CWPs, LWPs and IWPs were positively correlated with M2Modis, and the ori-

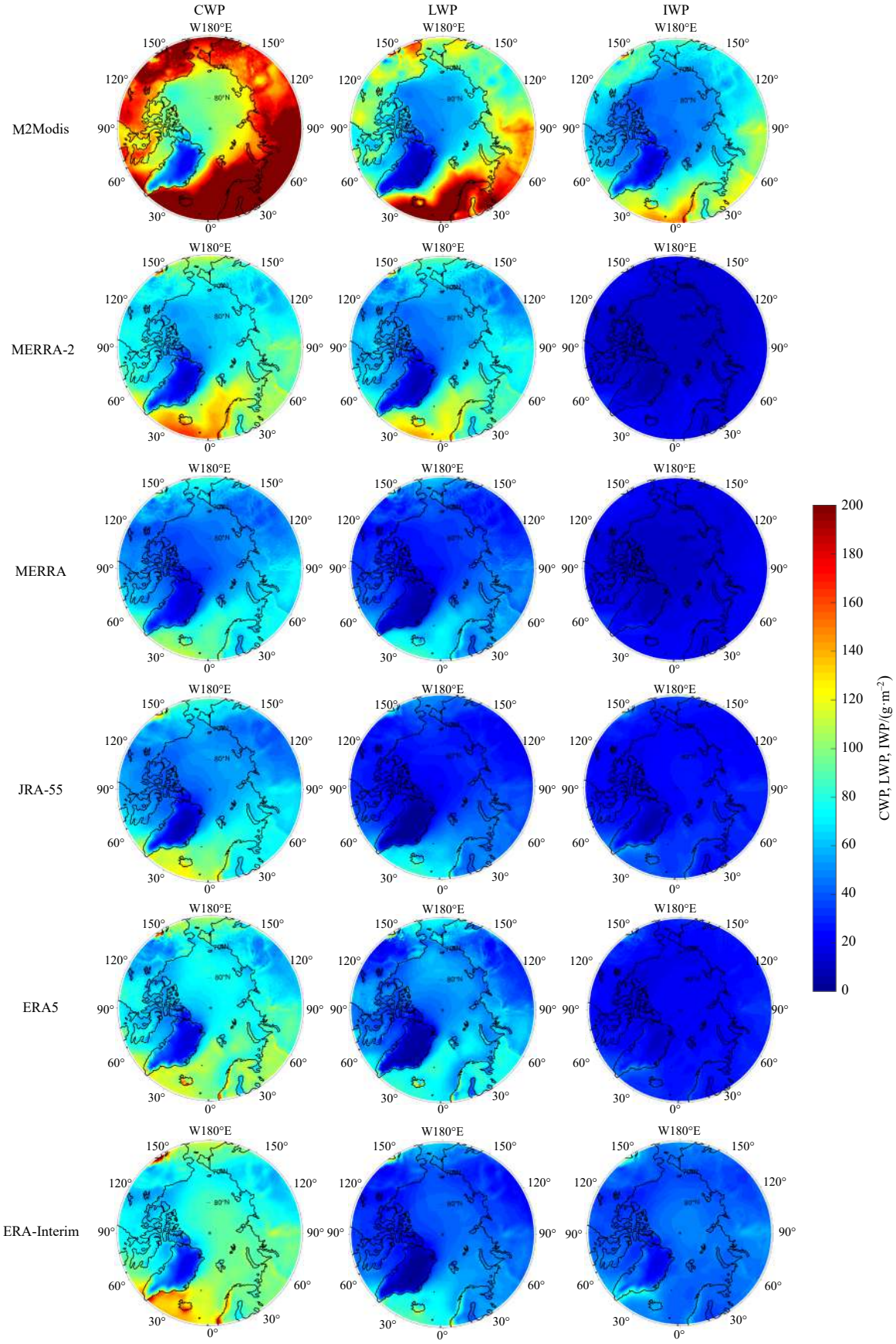

Fig. 1. Climatologies of the cloud water path (CWP, left column), the cloud liquid water path (LWP, middle column), and the cloud ice water path (IWP, right column) from M2Modis and the five reanalyses during the period of January 1980 to December 2015.

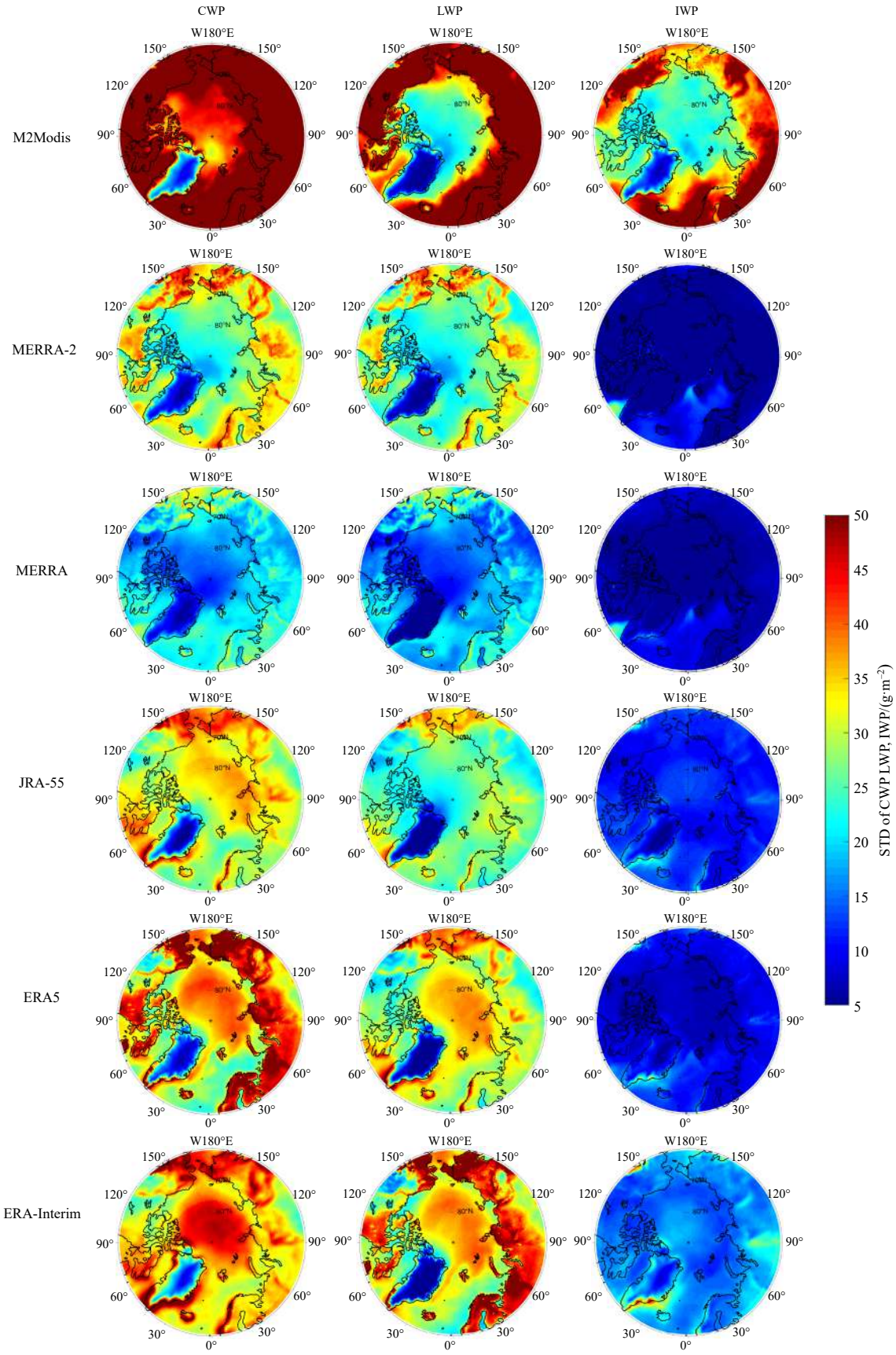

Fig. 2. Climatologies of standard deviations of the cloud water path (CWP, left column), the cloud liquid water path (LWP, middle column), and the cloud ice water path (IWP, right column) from M2Modis and the five reanalyses during the period of January 1980 to December 2015.

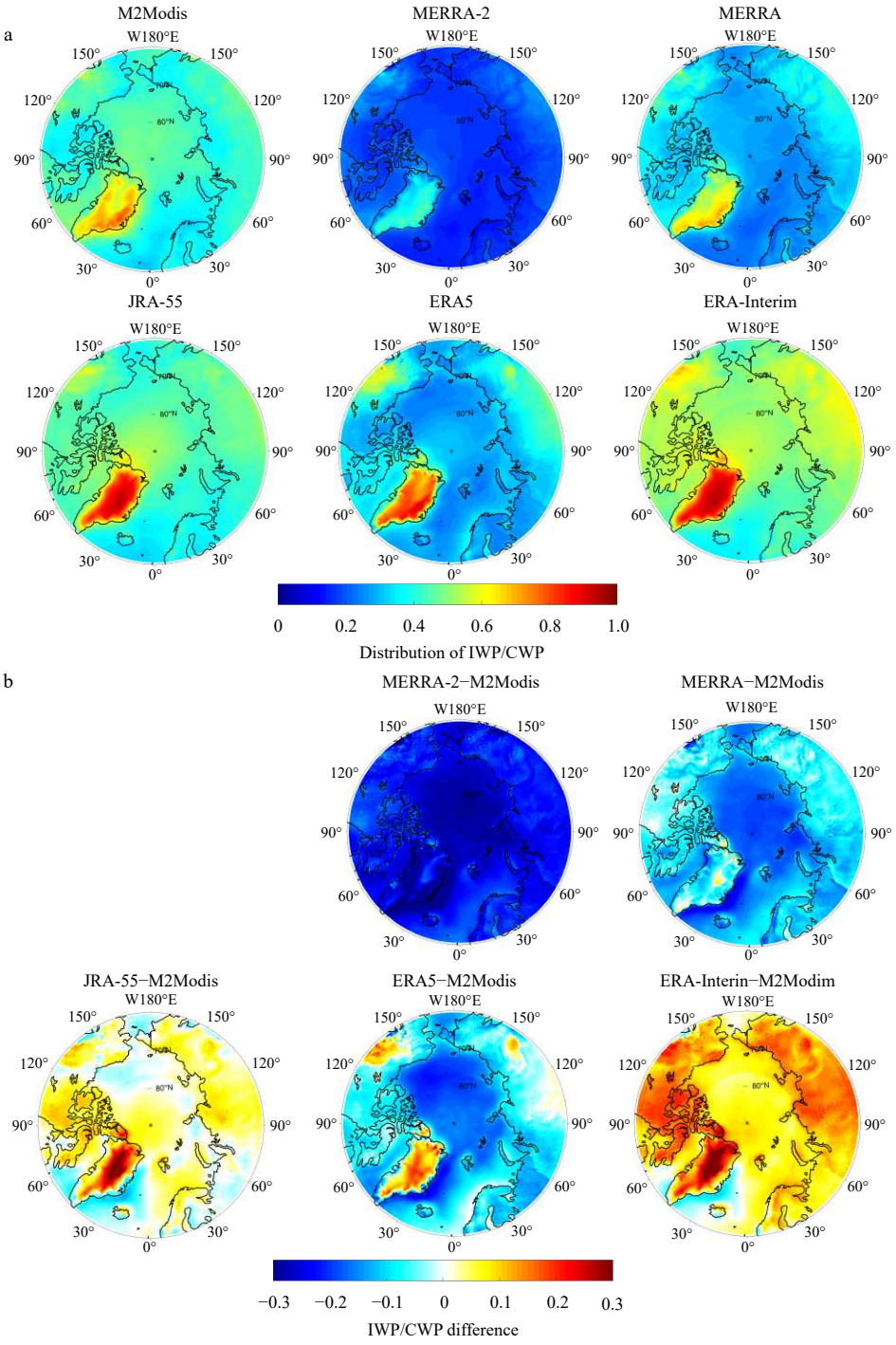

Fig. 3. Distributions of the IWP/CWP from M2Modis and the five reanalysis datasets (a), and differences between the five reanalysis datasets and M2Modis (b).

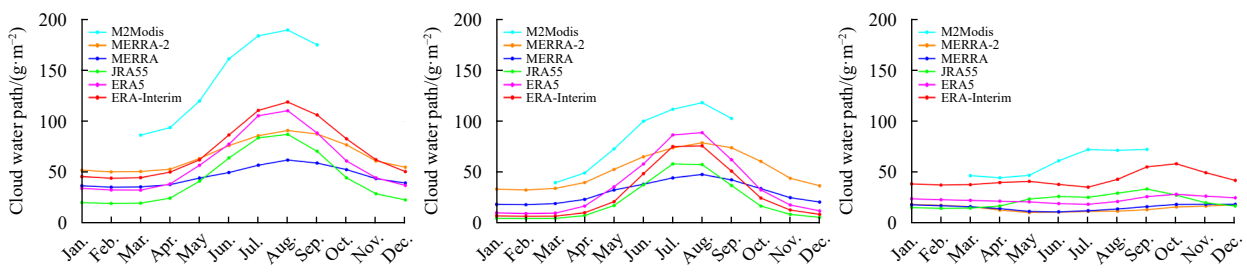

Fig. 4.

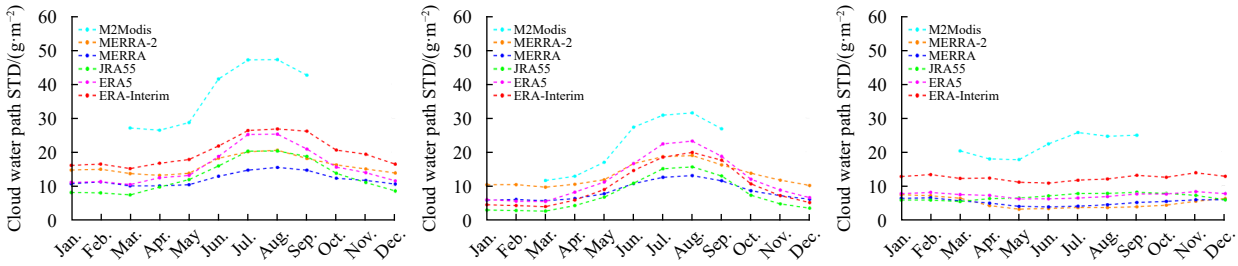

Fig. 4. Monthly means (first row) and monthly standard deviations (second row) of CWPs (left column), LWPs (middle column) and IWPs (right column) for different datasets.

ginal and detrended time series were statistically significant, except for the detrended ERA5 LWPs, suggesting that the interannual variability is consistent between M2Modis and the five reanalysis datasets.

4 Conclusions

This study has compared CWPs, LWPs, and IWPs of the five reanalysis datasets with the COSP output for Modis from MERRA-2 (M2Modis). The main conclusions are summarized

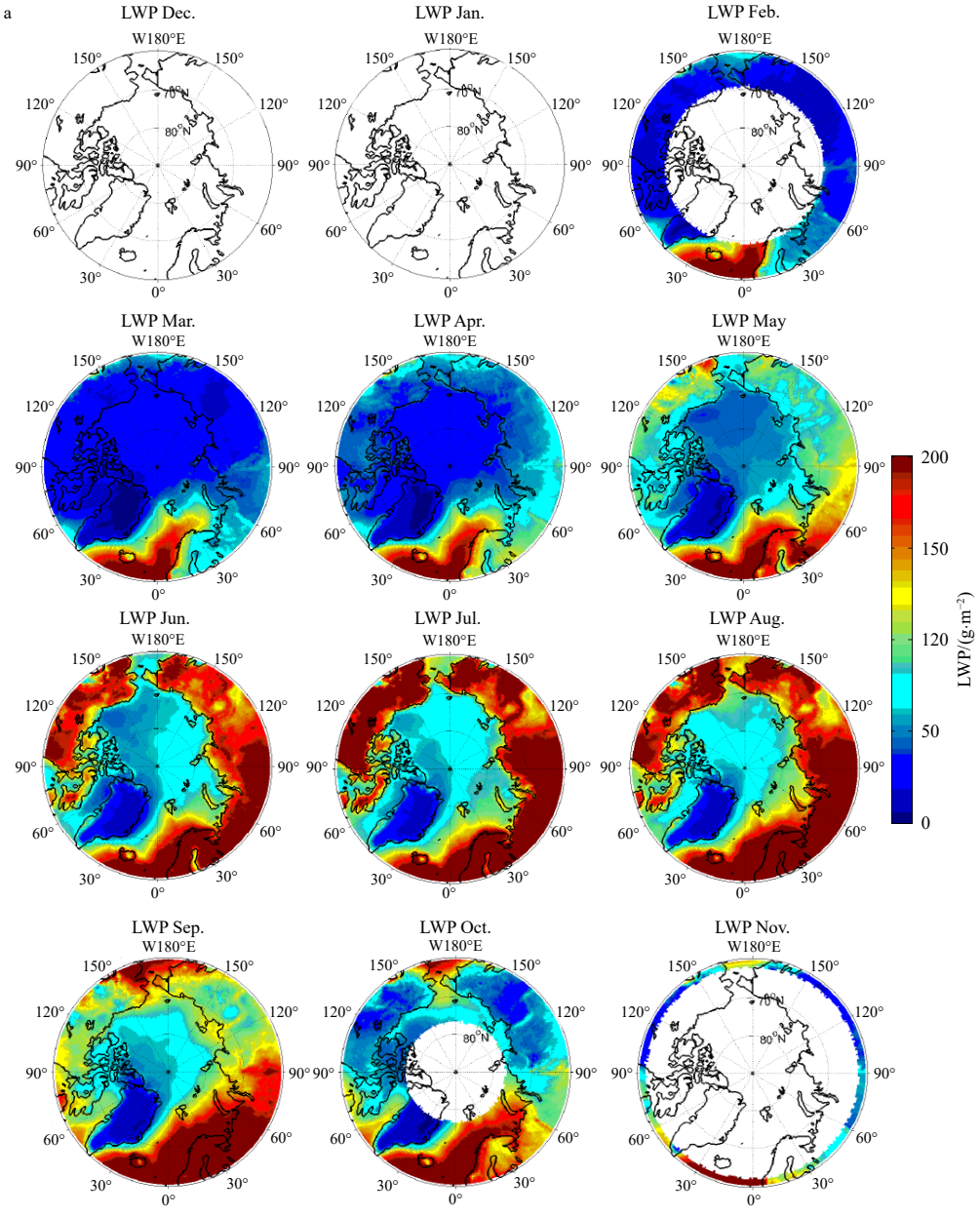

Fig. 5.

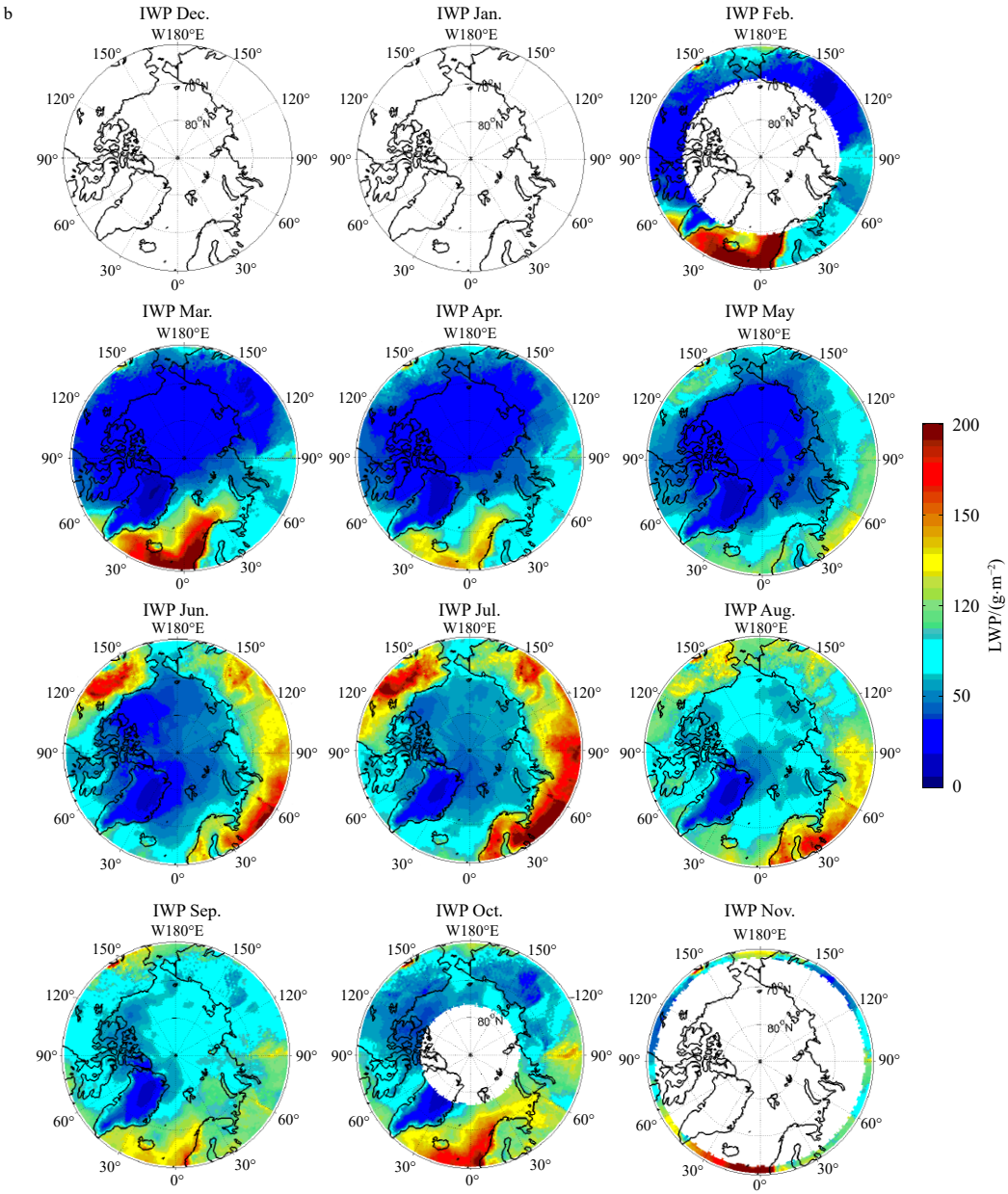

Fig. 5. Spatial distributions of the monthly mean (from December to November) LWPs (a) and IWPs (b) from M2Modis.

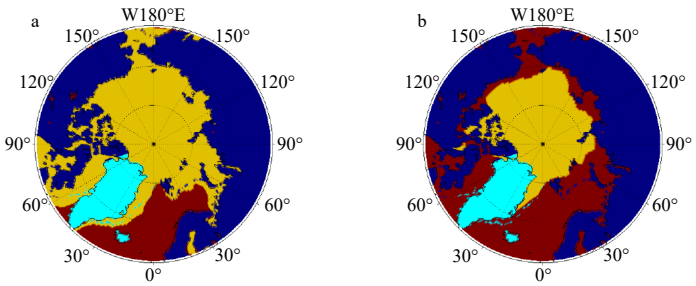

Fig. 6. Four sub-regions of the Arctic (Mainland: dark blue; Greenland: light blue; sea-ice-covered region: yellow, where monthly mean SIC ⩾15%; and ice-free ocean: dark red). a. March and b. September.

below.

(1) The climatological means and standard deviations of CWPs, LWPs, and IWPs of all reanalysis datasets are significantly different from those of M2Modis. The reanalysis data generally underestimate the climatological mean of the Arctic CWPs, LWPs, and IWPs. The CWPs in the reanalyzed data are only about half of those in M2Modis. Reanalysis data can capture relatively consistent regional differences in cloud water content in the Arc-

tic, i.e., small values over the central Arctic region, the central area of the North American continent, and eastern Eurasia, and large values over the Atlantic inflow region.

(2) The ratio of cloud liquid water to cloud solid water varies considerably among these datasets. MERRA-2 and MERRA underestimated this ratio, particularly for MERRA-2. ERA-Interim and JRA55 overestimated IWPs, especially over Greenland. In this regard, ERA5 outperforms the other reanalysis datasets. By comparing the performance and the cloud property parameterizations of two pairs of datasets, "ERA5 and ERA-Interim" and "MERRA and MERRA-2", we further found that the inclusion of re-evaporation processes increases the humidity in the atmosphere over the land (Figs 1 and 7) and that a more realistic liquid/ice phase can be obtained by treating the liquid and ice water contents independently (Fig. 3).

(3) The seasonal cycles of CWPs and LWPs from these data-

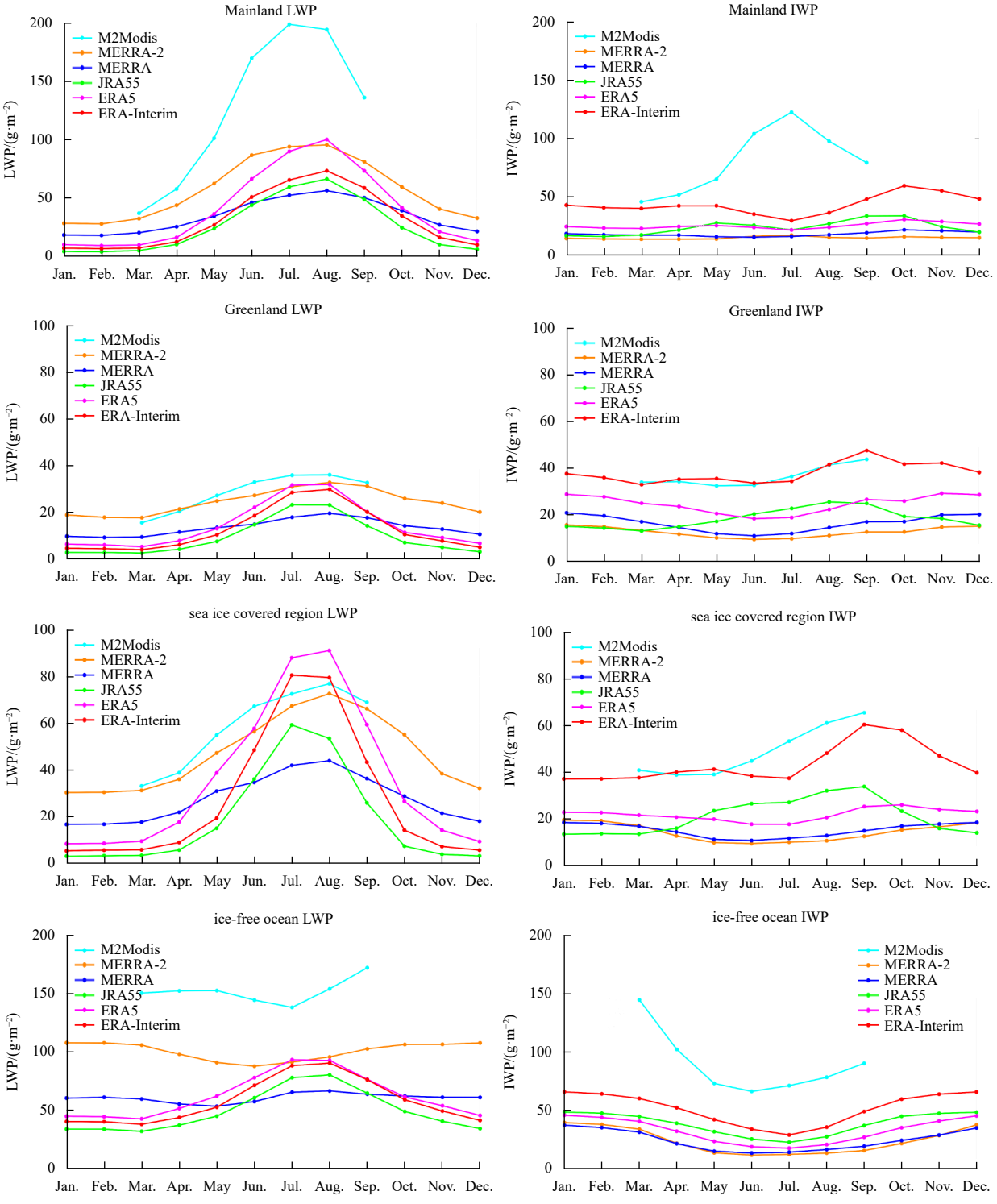

Fig. 7. Climatological seasonal cycles of LWPs (left column) and IWPs (right column) in four sub-regions of the Arctic (rows from top to bottom: Mainland, Greenland, sea-ice-covered region, and ice-free ocean).

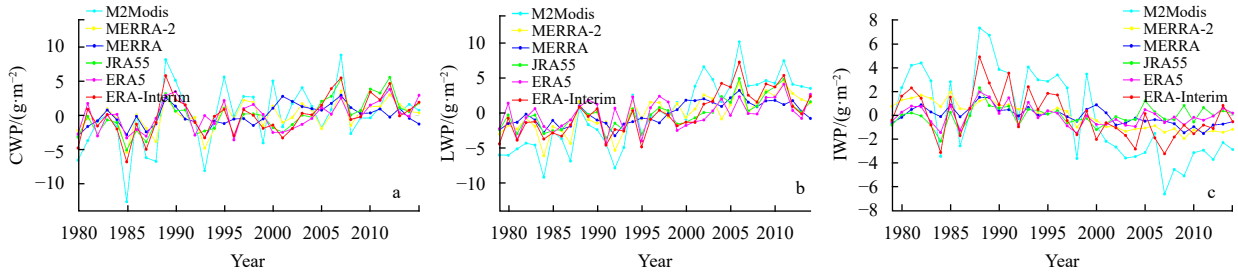

Fig. 8. Annual mean anomalies of CWPs (a), LWPs (b) and IWPs (c) from M2Modis and reanalysis datasets for the period of 1980–l2015.

Table 3. Linear trends in M2Modis and five reanalysis datasets, as well as correlation coefficients using original and detrended time series (in brackets) between M2Modis and each reanalysis dataset

Reanalysis datasets	CWP		LWP		IWP	
	Trend/(g·m^{-2}·century^{-1})	Corr/10^{-2}	Trend/(g·m^{-2}·century^{-1})	Corr/10^{-2}	Trend/(g·m^{-2}·century^{-1})	Corr/10^{-2}
M2Modis	22		42		–20	
MERRA-2	8	94(91)	18	95(83)	–9	86(87)
MERRA	6	67(61)	11	86(68)	–5	84(76)
ERA5	5	60(52)	8	57(33)	–2	74(73)
ERA–I	9	74(68)	17	84(62)	–7	82(75)
JRA–55	13	69(55)	12	84(60)	–8	40(57)

Note: Red color means passing the 95% significance test.

sets were similar, although the differences between their absolute values are large. There are higher CWPs and LWPs in summer than in winter; however, the seasonal cycles of IWPs are far from clear and consistent. IWPs from M2Modis have opposite seasonal variation over the land and ocean portions, i.e., small (large) in winter and large in summer over the land (ocean). The seasonal cycles of LWPs and IWPs from the five reanalysis datasets in the sub-regions show significant differences with respect to those of M2Modis. The largest difference for IWPs exists in July over Eurasia and North America.

(4) During the period of 1980–2015, no significant linear trends in CWPs, LWPs, and IWPs were found, except for LWP from M2Modis. However, increases in CWPs and LWPs and decreases in IWPs are consistent with Arctic warming. Another feature is that the results of all reanalysis datasets, except for ERA5 LWPs, have significant positive correlations with those from M2Modis for both original and detrended time series, suggesting a more consistent interannual variability between these datasets.

As found in this study, there are quite large differences in the cloud water paths between reanalysis datasets and M2Modis. It is a challenge to fully understand the causes. Here, the study offers some preliminary opinions that the study considers one of the reasons to be the biased nature of radiosonde humidity measurements in the Arctic, which makes it difficult to verify and adjust their cloud parameterization schemes in the Arctic (Dee et al., 2011). Some related processes like moisture intrusions can be captured by models, but the intensities and frequencies of these intrusions are often biased (Johansson et al., 2017; Liu et al., 2018). The Arctic mixed-phase cloud, the most frequently observed cloud type, is still not well understood and simulated (Qiu et al., 2015; Tan and Storelvmo, 2019). As shown in Table 1, the selected reanalysis systems use different cloud parameterizations to generate cloud properties. Different cloud properties can be generated even with the same water vapor and temperature. More specifically, differences in cloud condensation schemes may lead to large differences in cloud water content, and the choices of different cloud ice/water critical temperature can also lead to large differences in cloud liquid and solid water paths and their ratios. In view of the important role of Arctic clouds in the energy balance in the Arctic climate system, tremendous efforts will be required to reduce the uncertainties in cloud water paths in the Arctic.

Acknowledgements

We thank the groups of reanalyses for producing and making available their model output. All data used in this study are available online.

References

Bacmeister J T, Suarez M J, Robertson F R. 2006. Rain reevaporation, boundary layer-convection interactions, and pacific rainfall patterns in an AGCM. Journal of the Atmospheric Sciences, 63(12): 3383–3403, doi: 10.1175/JAS3791.1

Bosilovich M G, Lucchesi R, Suarez M. 2016. MERRA-2: File specification. GMAO Office Note No. 9 (Version 1.1). Greenbelt, Maryland: GMAO

Chernokulsky A, Mokhov I I. 2012. Climatology of total cloudiness in the arctic: an intercomparison of observations and reanalyses. Advances in Meteorology, 2012: 542093, doi: 10.1155/2012/542093

Chou M D, Suarez M J, Liang X Z, et al. 2001. A thermal infrared radiation parameterization for atmospheric studies. Technical Report Series on Global Modeling and Data Assimilation, NASA/TM-2001-104606, Vol. 19. Greenbelt, MD: Goddard Space Flight Center

Curry J A, Rossow W B, Randall D, et al. 1996. Overview of arctic cloud and radiation characteristics. Journal of Climate, 9(8): 1731–1764, doi: 10.1175/1520-0442(1996)009<1731:OOACAR>2.0.CO;2

Dee D P, Uppala S M, Simmons A J, et al. 2011. The ERA-Interim reanalysis: Configuration and performance of the data assimilation system. Quarterly Journal of the Royal Meteorological Society, 137(656): 553–597, doi: 10.1002/qj.828

Dethloff K, Handorf D, Jaiser R, et al. 2019. Dynamical mechanisms of Arctic amplification. Annals of the New York Academy of Sci-

ences, 1436(1): 184–194, doi: 10.1111/nyas.13698
Ebert E E, Curry J A. 1992. A parameterization of ice cloud optical properties for climate models. Journal of Geophysical Research: Atmospheres, 97(D4): 3831–3836, doi: 10.1029/91JD02472
ECMWF. 2010. IFS Documentation-CY36R1 Part IV: Physical Processes[J]. Reading, England: ECMWF, https://www.ecmwf.int/node/9233 [2010-1-26/2019-11-3], doi: 10.21957/2loi3bxcz
English J M, Kay J E, Gettelman A, et al. 2014. Contributions of clouds, surface albedos, and mixed-phase ice nucleation schemes to Arctic radiation biases in CAM5. Journal of Climate, 27(13): 5174–5197, doi: 10.1175/JCLI-D-13-00608.1
Fouquart Y. 1988. Radiative transfer in climate models. In: Schlesinger M E, ed. Physically-Based Modelling and Simulation of Climate and Climatic Change. Dordrecht: Springer, 223–283
Fu Q, Yang P, Sun W B. 1998. An accurate parameterization of the infrared radiative properties of cirrus clouds for climate models. Journal of Climate, 11(9): 2223–2237, doi: 10.1175/1520-0442(1998)011<2223:AAPOTI>2.0.CO;2
Gelaro R, McCarty W, Suárez M J, et al. 2017. The modern-era retrospective analysis for research and applications, version 2 (MERRA-2). Journal of Climate, 30(14): 5419–5454, doi: 10.1175/JCLI-D-16-0758.1
Geleyn J F, Hollingsworth A. 1979. An economical analytical method for the computation of the interaction between scattering and line absorption of radiation. Contrib to Atmospheric Physics, 52: 1–16
Hersbach H, Bell B, Berrisford P, et al. 2020. The ERA5 global reanalysis. Quarterly Journal of the Royal Meteorological Society, 146(730): 1999–2049, doi: 10.1002/qj.3803
Huang Y Y, Dong X Q, Xi B K, et al. 2017. Quantifying the uncertainties of reanalyzed Arctic cloud and radiation properties using satellite surface observations. Journal of Climate, 30(19): 8007–8029, doi: 10.1175/JCLI-D-16-0722.1
Johansson E, Devasthale A, Tjernström M, et al. 2017. Response of the lower troposphere to moisture intrusions into the Arctic. Geophysical Research Letters, 44(5): 2527–2536, doi: 10.1002/2017GL072687
Japan Meteorological Agency. 2019. Outline of the operational numerical weather prediction at the Japan Meteorological Agency. In: WMO Technical Progress Report on the Global Data-processing and Forecasting System and Numerical Weather Prediction. Japan: JMA, http://www.jma.go.jp/jma/jma-eng/jma-center/nwp/outline2019-nwp/index.htm [2019-3-30/2019-11-3]
Kay J E, L'Ecuyer T, Chepfer H, et al. 2016. Recent advances in arctic cloud and climate research. Current Climate Change Reports, 2(4): 159–169, doi: 10.1007/s40641-016-0051-9
Kobayashi S, Ota Y, Harada Y, et al. 2015. The JRA-55 reanalysis: general specifications and basic characteristics. Journal of the Meteorological Society of Japan Ser II, 93(1): 5–48, doi: 10.2151/jmsj.2015-001
Kitagawa H, Murai S. 2006. A revised radiation scheme for cloud treatments in the Japan Meteorological Agency Global Spectral Model. CAS/JSC WGNE Res. Activ Atmos Oceanic Modell, 36: 17–18
Lenaerts J T M, Van Tricht K, Lhermitte S, et al. 2017. Polar clouds and radiation in satellite observations, reanalyses, and climate models. Geophysical Research Letters, 44(7): 3355–3364, doi: 10.1002/2016GL072242
Li Z X, Le Treut H. 1992. Cloud-radiation feedbacks in a general circulation model and their dependence on cloud modelling assumptions. Climate Dynamics, 7(3): 133–139, doi: 10.1007/BF00211155
Liu Y H, Key J R. 2016. Assessment of arctic cloud cover anomalies in atmospheric reanalysis products using satellite data. Journal of Climate, 26(17): 6065–6083, doi: 10.1175/JCLI-D-15-0861.1
Liu Y H, Key J R, Vavrus S, et al. 2018. Time evolution of the cloud response to moisture intrusions into the Arctic during winter. Journal of Climate, 31(22): 9389–9405, doi: 10.1175/JCLI-D-17-0896.1
Martin G M, Johnson D W, Spice A. 1994. The measurement and parameterization of effective radius of droplets in warm stratocumulus clouds. Journal of the Atmospheric Sciences, 51(13): 1823–1842, doi: 10.1175/1520-0469(1994)051<1823:TMAPOE>2.0.CO;2
Molod A, Takacs L, Suarez M, et al. 2015. Development of the GEOS-5 atmospheric general circulation model: evolution from MERRA to MERRA2. Geoscientific Model Development, 8(5): 1339–1356, doi: 10.5194/gmd-8-1339-2015
Moorthi S, Suarez M J. 1992. Relaxed arakawa-schubert. a parameterization of moist convection for general circulation models. Monthly Weather Review, 120(6): 978–1002, doi: 10.1175/1520-0493(1992)120<0978:RASAPO>2.0.CO;2
Ou S C, Liou K N. 1995. Ice microphysics and climatic temperature feedback. Atmospheric Research, 35(2–4): 127–138
Qiu S Y, Dong X Q, Xi B K, et al. 2015. Characterizing Arctic mixed-phase cloud structure and its relationship with humidity and temperature inversion using ARM NSA observations. Journal of Geophysical Research: Atmospheres, 120(15): 7737–7746, doi: 10.1002/2014JD023022
Räisänen P. 1998. Effective longwave cloud fraction and maximum-random overlap of clouds: A problem and a solution. Monthly Weather Review, 126(12): 3336–3340, doi: 10.1175/1520-0493(1998)126<3336:ELCFAM>2.0.CO;2
Rienecker M M, Suarez M J, Gelaro R, et al. 2011. MERRA: NASA's modern-era retrospective analysis for research and applications. Journal of Climate, 24(14): 3624–3648, doi: 10.1175/JCLI-D-11-00015.1
Rozenhaimer M S, Barton N, Redemann J, et al. 2018. Bias and sensitivity of boundary layer clouds and surface radiative fluxes in MERRA-2 and airborne observations over the Beaufort Sea during the ARISE campaign. Journal of Geophysical Research: Atmospheres, 123(12): 6565–6580, doi: 10.1029/2018JD028349
Savijärvi H, Räisänen P. 1998. Long-wave optical properties of water clouds and rain. Tellus A, 50(1): 1–11, doi: 10.3402/tellusb.v50i1.16018
Screen J A, Simmonds I. 2010. The central role of diminishing sea ice in recent Arctic temperature amplification. Nature, 464(7293): 1334–1337, doi: 10.1038/nature09051
Serreze M C, Barry R G. 2011. Processes and impacts of Arctic amplification: a research synthesis. Global and Planetary Change, 77(1–2): 85–96, doi: 10.1016/j.gloplacha.2011.03.004
Slingo A. 1989. A GCM parameterization for the shortwave radiative properties of water clouds. Journal of the Atmospheric Sciences, 46(10): 1419–1427, doi: 10.1175/1520-0469(1989)046<1419:AGPFTS>2.0.CO;2
Sommeria G, Deardorff J W. 1977. Subgrid-scale condensation in models of nonprecipitating clouds. Journal of the Atmospheric Sciences, 34(2): 344–355, doi: 10.1175/1520-0469(1977)034<0344:SSCIMO>2.0.CO;2
Tan I, Storelvmo T. 2019. Evidence of strong contributions from mixed-phase clouds to arctic climate change. Geophysical Research Letters, 46(5): 2894–2902, doi: 10.1029/2018GL081871
Taylor P C, Boeke R C, Li Y, et al. 2019. Arctic cloud annual cycle biases in climate models. Atmospheric Chemistry and Physics, 19(13): 8759–8782, doi: 10.5194/acp-19-8759-2019
Tiedtke M. 1993. Representation of clouds in large-scale models. Monthly Weather Review, 121(11): 3040–3061, doi: 10.1175/1520-0493(1993)121<3040:ROCILS>2.0.CO;2
Walsh J E, Chapman W L, Portis D H. 2009. Arctic cloud fraction and radiative fluxes in atmospheric reanalyses. Journal of Climate, 22(9): 2316–2334, doi: 10.1175/2008JCLI2213.1
Wang Z M, Zhang X D, Guan Z Y, et al. 2015. An atmospheric origin of the multi-decadal bipolar seesaw. Scientific Reports, 5: 8909, doi: 10.1038/srep08909
Washington W M, Williamson D L. 1977. A description of the NCAR global circulation models. National Center for Atmospheric Research Ncar Koha Opencat, 17: 111–172, doi: 10.1016/b978-0-12-460817-7.50008-2